Applied Energy 261 (2020) 114434

Contents lists available at ScienceDirect

Applied Energy

journal homepage: www.elsevier.com/locate/apenergy

Study of the effects of axial conduction on the performance of thermoelectric generators integrated in a heat exchanger for waste heat recovery applications

M.H. Zaher, M.Y. Abdelsalam, J.S. Cotton*

Department of Mechanical Engineering, McMaster University, Hamilton, Ontario L8S 4L7, Canada

HIGHLIGHTS

- Numerical study of heat exchangers with integrated thermoelectric generators (TEGs).
- Axial conduction has an adverse effect on TEGs power output in heat exchangers.
- Improved TEGs power output (up to 20%) is obtained by reducing axial conduction.
- Introduction of "Power Gain" term to represent enhancement in TEGs power output.
- Novel design and sizing criteria are introduced for TEG integrated heat exchangers.

ARTICLE INFO

Keywords:
Waste heat recovery
Thermoelectric generators
TEG
Heat exchangers
Design criteria
Axial conduction
Exhaust gas
Analytical modeling
Low temperature commercial applications

ABSTRACT

The electrical power generated from thermoelectric generators (TEGs) integrated in a heat exchanger is maximized by applying novel heat exchanger design criteria for waste heat recovery systems. A numerical model is developed and experimentally validated to simulate the performance of TEG-integrated heat exchangers. The performance of a heat recovery system, suitable for low temperature commercial applications ~300 °C, is investigated for a range of heat exchanger sizes of 2 to 8 TEG rows and exhaust gas mass flow rates of 0.02 to 0.08 kg/s. The adverse effect of the heat conducted axially, along the flow direction, on the total power output of the TEGs is quantified. The number of rows reaches an optimum value for a given gas flow rate beyond which a significant drop in the hot-side temperature of the upstream TEG rows occurs due to the increase of the axial conduction between successive rows. The term "Power Gain" is introduced in this study as the ratio between the power output from a system without axial conduction to that with axial conduction. Power Gain shows the potential benefits of limiting the axial conduction through the heat exchanger and values up to 1.2 times (20% increase in power) can be obtained for relatively low exhaust gas flow rates (~0.02 kg/s). Novel performance maps are developed to correlate the power output with the heat exchanger design, exhaust gas flow rate and number of TEGs. Such maps can be used to guide the optimization of the design of TEG-integrated waste heat recovery systems.

1. Introduction

Waste heat recovery systems are crucial to the harvesting of the unutilized thermal energy in the exhaust streams of various commercial and industrial processes. The exponential increase in the global energy demands always raises concerns about the exacerbating issue of climate change. Major energy savings can be obtained from the repurposing of waste heat into useful forms to meet a portion of the energy demand (i.e., electrical and/or thermal). As such, proper designs of waste heat recovery systems help achieve more efficient utilization of energy, and hence considerable reductions in the fossil fuel consumption and the associated harmful greenhouse gas emissions. One example of such systems is the thermoelectric generator (TEG), which is a solid-state device that consists of p- and n-type semiconductors joined together to form an electric circuit. While operating under a temperature difference, the TEG converts the heat flow into electric power by virtue of the Seebeck effect. Generation of electrical power using TEGs has become a viable option compared to other conventional systems owing to their reliable and maintenance-free operation as well as their favorable performance under low temperature differences [1].

* Corresponding author.

https://doi.org/10.1016/j.apenergy.2019.114434
Received 13 September 2019; Received in revised form 18 December 2019; Accepted 19 December 2019
Available online 06 January 2020
0306-2619/

Nomenclature

Latin Letters

I	Current Output [A]
K	Thermal Conductance [W/K]
P	Power Output [W]
Q	Heat Transfer Rate (Flow) [W]
r, R	Electrical Resistance [ohm]
R_{th}	Thermal Resistance [K/W]
T	Temperature [°C or K]
V	Voltage Output [V]

Greek Letters

α	Seebeck Coefficient [V/K]
ε	Joule Heat Distribution Ratio [–]
ϵ	effectiveness [–]
η	Efficiency [–]
λ	Thermal Conductivity [W/m K]

Subscripts

A	Axial
av	Average
cd	Conductor
c, ct	Contact
C	Cold-side
g	Gas
G	Gap
H	Hot-side
m	Row/Element Number
n	Node Number
th	Thermal
T	Thermoelectric Generator (TEG)
w	Water

Acronyms

AC	Axial Conduction
HX	Heat Exchanger
NAC	No Axial Conduction
TEG	Thermoelectric Generator
TEG-HX	TEG Integrated Heat Exchanger

Waste heat is generated from processes of heating or power generation in the form of exhaust gases at elevated temperatures that are typically discharged into the atmosphere. Integrating heat exchangers between such exhaust streams and the hot side of TEGs enables the generation of useful electrical power. However, the efficient operation of the system requires a cooler fluid stream acting as a heat sink at the cold side of the TEGs. In order to design and size such a system for waste heat recovery, accurate modeling of the performance of the TEGs and the heat transfer mechanisms through the heat exchanger is required. The performance of the TEG can be evaluated by modeling the heat and current flows through the TEG using the thermoelectric properties of the TEG material. Several modeling methodologies for TEGs have been investigated in the literature such as idealized steady-state models [2,3], and models including the effect of the electrical contact resistance on the performance [4] as well as the effect of temperature-dependent thermoelectric properties [5,6]. The heat transfer mechanisms through the heat exchanger include convection between the exhaust gas and the heat exchanger hot surface, conduction through the heat exchanger structure and the contacts at the TEG surfaces, and convection between the coolant stream and the heat exchanger cold surface. Thermal resistances associated with these heat transfer mechanisms have a critical effect on the performance of the TEGs since they directly impact the temperature differences between the heat source/sink and the TEG hot/cold surfaces, respectively. Furthermore, the flow rates through both sides of the heat exchanger have a major influence on the effectiveness of the heat exchanger pronounced in the streamwise temperature variation of the heat source/sink flows. Several studies assumed uniform temperatures for the heat source and sink and studied the performance of TEGs in a heat exchanger under the effect of varying the TEG geometrical parameters using a simplified model. Henderson [7] and Stevens [8] studied the effect of the length of the TEG elements on the power output under low temperature difference. Min and Rowe [9,10] studied the optimization of the TEG module geometry. Rowe et al. [11,12] investigated the performance of TEG modules under the effect of the thermal resistance of the heat transfer medium. A simplified model was used in [13,14], referred to as the "first-level model", where the current flow through the TEG was neglected, thereby omitting the effects of the Peltier and Joule heating. Freunek et al. [15,16] investigated the effect of the heat exchanger thermal resistance on load matching. The study showed that the matched load occurred at an effective internal resistance that was higher than the calculated internal resistance of the TEG due to the effect of the heat exchanger thermal resistances. This was often neglected in the literature [13,17,18] and was shown to cause deviations in the estimated power output, voltage and current. Different heat exchanger models were explored to simulate the effect of temperature variation along the flow direction on the performance of TEGs integrated in the heat exchanger design. A numerical model was developed by Crane et al. [19] to simulate the performance of TEGs in an automotive waste heat recovery system. The analysis considered the axial heat conduction (i.e., the heat conducted axially through the walls of the heat exchanger in the direction of the flow). The heat exchanger was discretized into cells along the direction of the hot fluid flow and the energy equations were solved iteratively using Newton-Raphson method. The model was validated experimentally for TEG modules integrated in a heat exchanger with hot water and cooling air channels [20]. Although the axial conduction was considered, its impact on the power output of the TEGs was not investigated. Kumar et al. [17,18] developed a numerical model for TEGs in a parallel plate-fin heat exchanger for automotive waste heat recovery. The flow domain was discretized along the exhaust flow direction. The temperature-dependent thermoelectric properties were averaged over the range of operating temperatures of each of the TEG junctions, and the model equations were then solved iteratively. The study used a 1-D thermal network and the axial conduction through the heat exchanger walls was not considered. In addition, the effective electrical internal resistance of the TEG was ignored in the external load matching. A parallel-plate heat exchanger with thermoelectric generator was modelled numerically by Yu et al. [21] to explore the effect of the flow temperature profiles and flow rates on the performance of the TEGs. The model was validated experimentally by Niu et al. [22] for low temperature waste heat recovery system. The numerical model was found to over-predict the power output and efficiency of the system over the entire range of heat source inlet temperatures. The discrepancy was attributed to the thermal losses from the heat exchanger to the surroundings in addition to the temperature dependence of the thermoelectric properties which were not considered in the model [22]. Furthermore, the axial heat conduction between the TEGs was neglected which contributed to the deviation in the predicted

power output. Similarly, Gou et al. [23] has also presented a simplified model where the temperature distribution along the TEG modules and the axial conduction of heat through the flow channel and the heat sinks were neglected. Hsu et al. [24] tested the effect of the temperature uniformity of the hot-side surface of an array of TEGs on the performance of the TEG system. Meng et al. [25] investigated the optimization of TEGs for automobile exhaust waste heat recovery considering the temperature variation along the flow direction in the exhaust and coolant channels. The performance of the TEG module was evaluated numerically while operating under different values of electric current and using different numbers of TEGs per module. By increasing the number of TEGs in the exhaust direction, the total output power was shown to increase up to an optimum of 16 TEGs then decreased. The output power of the individual TEGs in the module was found to decrease by increasing the number of TEGs per module. This was due to the axial heat conduction in the exhaust channel wall which caused the hot side temperature of the upstream TEGs to drop as more were introduced downstream [25]. Zaher [26] studied the optimization of TEG geometrical parameters under the effect of axial conduction on the temperature distribution along a multi-row heat exchanger. The study showed a decrease in the TEGs total power due to axial conduction. In addition, it was shown that the thickness of the TEG (i.e. the length of the thermo-electric element in the direction of the heat flow) has a critical impact on the power output. Transient TEG heat exchanger models were developed to investigate the TEG performance under varying exhaust conditions for automotive applications [24,25,27]. Wang et al. [28] developed a transient model to investigate the optimization of the number of TEG elements and the height of the thermoelements for an automotive waste heat recovery system. The axial conduction within the heat exchanger was not considered in the model. Love et al. [29] studied the performance of TEGs under the effect of fouling for different heat exchanger materials for vehicles exhaust gas recirculation (EGR) systems.

Large amounts of thermal energy is constantly wasted from gas-fired appliances in food industry with temperature levels up to 400 °C [1]. As such, this offers a great potential for electricity generation using thermoelectric generators (TEGs) in waste heat recovery systems [25,30]. Although the efficiency of TEGs is relatively low for this temperature range, the power output from the waste heat recovery system is considered more valuable than the efficiency since waste heat can be considered as a free source of energy [12]. Few researchers [26,30–32] designed and tested waste heat recovery systems with integrated TEGs for commercial food industry applications. These systems were meant to harvest the thermal energy wasted from natural-gas-fired ovens with naturally ventilated exhaust stream [32]. The oven was operated continuously to maintain a temperature of 260 °C for baking purposes. As a result, heat was lost at a rate of approximately 10 kW through the chimney to the outdoor atmosphere. Girard [32] studied the influence of introducing the waste heat recovery system at the inlet of the chimney of the oven. The study showed that the waste heat recovery system impeded the natural draft through the oven by reducing the inlet temperature to the chimney. This resulted into potential reduction of the natural gas consumption by the oven of around 13% with no effect on the operation of the oven.

As observed from the previous studies, the integration of TEGs in waste heat recovery applications has been the topic of interest of researchers and engineers for the efficient utilization of the recovered thermal energy by directly converting it to electricity. Within the current state-of-the-art, the optimization of the designs of the heat exchanger and the TEG modules has been widely considered. However, the understanding of the unfavorable effect of heat conduction in the axial direction (i.e. in the flow direction) on the TEGs performance seemed to be lacking. As such, the main objective of this article is set to study the adverse effect of axial heat conduction on the performance of TEG-integrated heat exchangers and to develop novel criteria to guide their design and sizing for waste heat recovery applications. A numerical model is developed for the TEG-integrated heat exchanger system and the numerical results are validated using experimental results presented by Girard [32]. The model takes into consideration the effects of the streamwise variation of the temperature of the heat source and sink, the electrical connections between the TEGs, the electrical load matching and the axial heat conduction through the structure of the heat exchanger. The term “Power Gain” is introduced to illustrate the difference between the system performance with and without the effect of the axial heat conduction in the heat exchanger. Performance maps are then developed for the cases with and without the axial conduction to correlate between the heat exchanger effectiveness, the exhaust mass flow rate, the number of TEGs, and the power output. Such maps are useful to guide decisions at the design stage about the optimum sizing of the heat exchanger with an integrated TEG system (TEG-HX) as well as the techno-economic value of limiting the axial conduction between consecutive TEG rows on the heat exchanger.

2. Numerical Modeling of TEG-integrated Heat Exchanger

A numerical model is developed to study the performance of TEGs in a multi-row heat exchanger at different operating conditions and evaluate the effect of the axial heat conduction between consecutive TEG rows. The heat exchanger is assumed to operate between exhaust gas acting as the heat source, and water acting as the heat sink as shown in the schematic in Fig. 1. The model takes into consideration the coupling between the heat conduction through the TEGs, the Peltier and Joule heating effects due to the electric current flow through the TEGs, and the convection thermal resistances of the gas and water flows through the heat exchanger. The flow domains of the heat source and sink and the heat exchanger are discretized in the axial direction (i.e., the direction of the flow). A thermal network, shown in Figs. 2a and 2b, is created to model the performance of multiple rows of TEGs connected electrically in series. Each TEG row is discretized into several elements (N_E) in the direction of the exhaust gas flow.

Consider Fig. 2b, on the exhaust gas side, the streamwise temperature distribution of the exhaust gas and the hot side of the heat exchanger are given as $T_{g,n}$ and $T_{H,m}$. The average hot-side temperature of the TEG element is represented by $T_{T,H,m}$. Similarly, on the coolant side, the streamwise temperature distribution of the coolant and the cold side of the heat exchanger are given as $T_{W,n}$ and $T_{C,m}$, respectively. The average cold-side temperature of the TEG element is represented by $T_{T,C,m}$. The thermal conductance values due to convective heat transfer (normal to the direction of flow) in the exhaust gas and the coolant flows are given as $K_{H,m}$ and $K_{C,m}$, respectively. The thermal conductance values due to the axial conduction through the hot- and cold-side heat exchangers are denoted by $K_{A,H,n}$ and $K_{A,C,n}$, respectively. The thermal resistances due to the contact between the heat exchangers and the TEGs are accounted for in the terms $K_{Ct,H,m}$ and $K_{Ct,C,m}$. For a given TEG row, multiple TEG modules can be installed side by side. The thermal conductance for the air gap between the TEGs in the same row is $K_{G,m}$, whereas the value of $K_{T,m}$ represents the thermal conductance

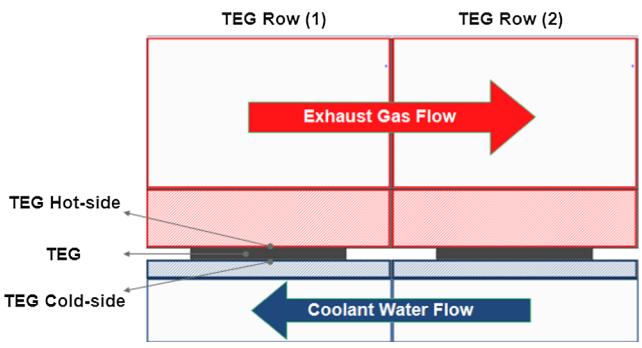

Fig. 1. Schematic of a TEG-HX.

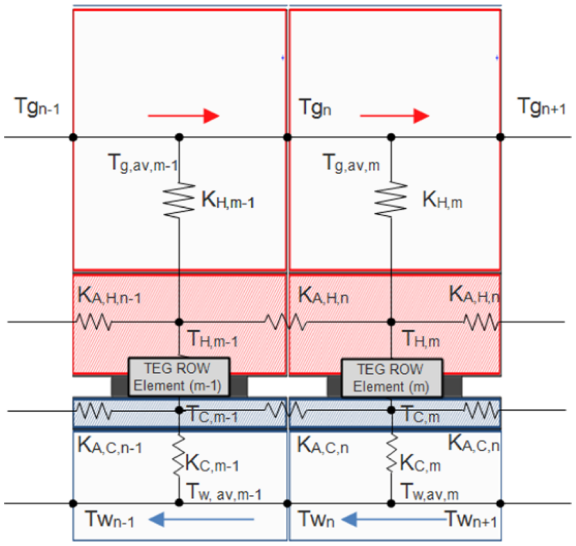

Fig. 2a. Thermal network of a single row discretized into 2 elements.

of the TEG element. The components of Joule heating that are transferred into the hot- and cold-sides of the TEG are given as $\varepsilon I_m^2 r_{T,m}$ and $(1-\varepsilon) I_m^2 r_{T,m}$, respectively, where $r_{T,m}$ is the internal electrical resistance of the TEG. For flat TEGs, the value of the distribution ratio of the Joule heating (ε) was found to be equal to 0.5 [16]. The components of the Peltier effect are given as functions of the hot and cold-side temperatures as $\alpha_T I_m T_{H,m}$ and $\alpha_T I_m T_{C,m}$, respectively, where α_T is the Seebeck coefficient.

The energy balance under steady state operation can be represented using the following equations:

Heat balance on the exhaust gas flow:

$$\dot{m}_g C_{p,g}(T_{g,n} - T_{g,n+1}) = K_{H,m}\left(\frac{T_{g,n} + T_{g,n+1}}{2} - T_{H,m}\right) \tag{1}$$

Heat balance on the wall in contact with the TEGs Hot-side:

$$K_{H,m}\left(\frac{T_{g,n} + T_{g,n+1}}{2} - T_{H,m}\right) = K_{Ct,H,m}(T_{H,m} - T_{TH,m}) \tag{2}$$

Heat balance on the TEGs hot-side:

$$K_{Ct,H,m}(T_{H,m} - T_{TH,m}) = K_{T,m}(T_{T,H,m} - T_{TC,m}) + \alpha_{T,m} I_m T_{T,H,m} - \varepsilon I_m^2 r_{T,m} + K_{G,m}(T_{T,H,m} - T_{T,C,m}) \tag{3}$$

Heat balance on the TEGs cold-side:

$$K_{Ct,C,m}(T_{T,C,m} - T_{C,m}) = K_{T,m}(T_{T,H,m} - T_{TC,m}) + \alpha_{T,m} I_m T_{T,C,m} + (1-\varepsilon) I_m^2 r_{T,m} + K_{G,m}(T_{T,H,m} - T_{T,C,m}) \tag{4}$$

Heat balance on the wall in contact with the TEGs cold-side:

$$K_{C,m}\left(T_{C,m} - \frac{T_{w,n} + T_{w,n+1}}{2}\right) = K_{Ct,C,m}(T_{T,C,m} - T_{C,m}) \tag{5}$$

Heat balance on the water flow:

$$\dot{m}_w C_w (T_{w,n+1} - T_{w,n}) = K_{C,m}\left(T_{C,m} - \frac{T_{w,n} + T_{w,n+1}}{2}\right) \tag{6}$$

The performance of the TEG-HX can be evaluated by solving for the temperatures numerically, using different values of current (I_m). The model is solved iteratively to evaluate the temperatures of the thermal nodes in the network for known inlet exhaust gas and cooling water temperatures. The thermal network of a single element of TEG, shown in Figs. 2a and 2b, is used as a building block in the multi-row TEG-HX model to evaluate the performance of a heat exchanger consisting of multiple rows of TEGs under steady-state operating conditions. The rows are connected thermally through the gas flow, the water flow and the heat exchanger structure. Also, they are connected electrically through the electrical connections between the TEGs either in series or in parallel configuration. The thermal/electrical network for the multi-row TEG-HX assembly is shown in Fig. 3.

As shown in Fig. 3, the hot-sides of the TEGs are represented by the nodes with temperature (T_H), while the cold-sides are represented by the nodes with temperature (T_C). An axial heat conduction component was added to the heat transfer equations of the TEG hot-side and cold-side surfaces to account for the heat conducted though the heat exchanger structure. Eqs. (2) and (5) can be rewritten as:

$$K_{H,m}\left(\frac{T_{g,n} + T_{g,n+1}}{2} - T_{H,m}\right) = K_{A,H,n+1}(T_{H,m} - T_{H,m+1}) - K_{A,H,n}(T_{H,m-1} - T_{H,m}) + K_{Ct,H,m}(T_{H,m} - T_{TH,m}) \tag{7}$$

$$K_{C,m}\left(T_{C,m} - \frac{T_{w,n} + T_{w,n+1}}{2}\right) = K_{A,C,n+1}(T_{C,m} - T_{C,m+1}) - K_{A,C,n}(T_{C,m-1} - T_{C,m}) + K_{Ct,C,m}(T_{T,C,m} - T_{C,m}) \tag{8}$$

At the beginning of the solution, the temperature values of all the thermal nodes on the exhaust gas and the cooling water sides are assumed to be the same as the inlet temperatures. After each iteration, the solution of thermal network shown in Fig. 3 is obtained to resolve the thermal coupling between the adjacent rows and update the values from previous iterations. The error in the overall energy balance of the heat exchanger and the absolute difference in the temperature of the thermal nodes between successive iterations are used to indicate the

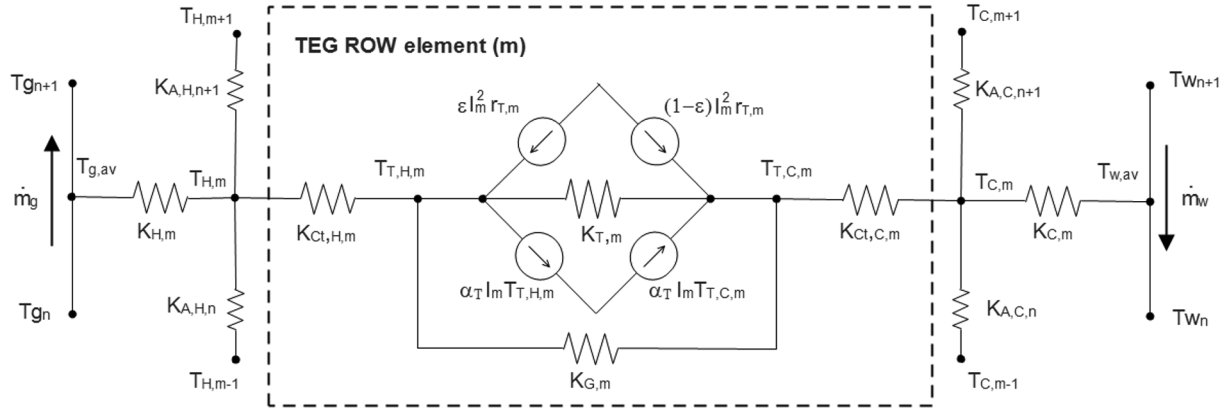

Fig. 2b. Description of the thermal network for a discretized element of TEG-HX.

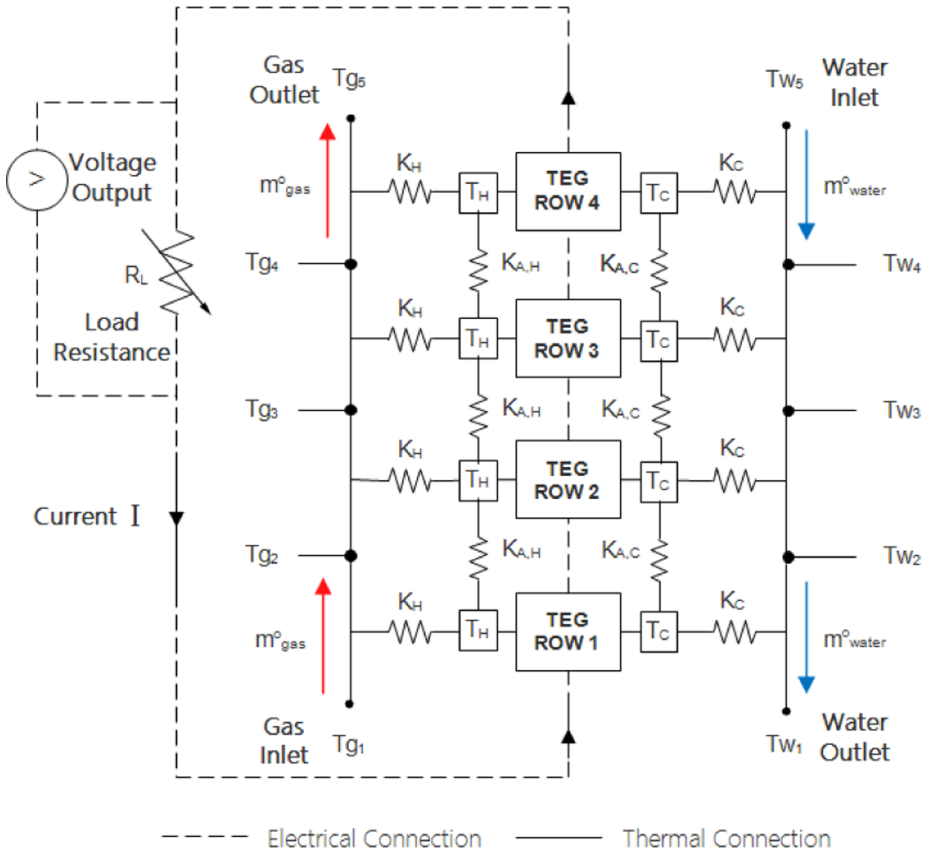

Fig. 3. Description of a thermal/electrical network for 4-row TEG module integrated in a heat exchanger.

convergence of the numerical solution. The convergence of the solution is assumed when the maximum error is less than 10^{-5}.

The electrical output of the TEGs is evaluated numerically for different values of current (I_m) using the following equations:

$$V = \alpha_{T,m}(T_{TH,m} - T_{TC,m}) - I_m r_{T,m} \quad (9)$$

$$P = \alpha_{T,m} I_m (T_{TH,m} - T_{TC,m}) - I_m^2 r_{T,m} \quad (10)$$

The electrical output solution is dependent on the electrical configuration of the TEG rows, i.e. series or parallel. After the thermal network solution is obtained, the electrical output is calculated using the voltage and current outputs of each TEG row. Different solution conditions are required for each type of electrical configuration; a series connection between the TEG rows dictates equal current in all rows, whereas a parallel connection dictates equal voltage across all rows.

In order to evaluate the effect of the temperature profiles of the exhaust gas and the axial conduction on the performance of the system, some assumptions are made to simplify the analysis:

1) All properties are assumed independent of the temperature.
2) Steady-state operation is assumed for the system and average flow rates are considered for the exhaust gas and cooling water.
3) Negligible thermal losses from the gas flow and the heat exchanger to the atmosphere.
4) The average fluid temperature is considered between the inlet and outlet of the flow at each element as shown in Figs. 1 and 2.
5) For the hot-side heat exchanger, the gas flow is assumed to have a uniform temperature and velocity distribution in the plane perpendicular to the exhaust flow direction. The flow is also assumed to be fully developed.
6) For the cold-side heat exchanger, the water flow rate and inlet temperature are assumed constant per row of TEGs.
7) The gap between the TEGs is assumed to be filled with thermally-insulating material and the heat transfer through it is assumed negligible.
8) Average temperature is used to evaluate heat flow and power output at each node of each discrete element (m).

Each row of TEGs was discretized into 20 elements ($\Delta x = 3.15mm$)for refined temperature profiles. A sensitivity analysis shows that increasing the number of discretization elements per TEG row (N_E) from 1 to 4 elements led to a maximum change in the temperature distribution of 1%.

3. Experimental Validation of the Numerical Model

The multi-row TEG-HX model is validated using the experimental results presented by Girard [32] and Zaher [26] for a double-row TEG-HX waste heat recovery system integrated into the chimney of a commercial oven, as described in Appendix A. A plate-fin HX was designed on the exhaust side, whereas an impinging water-jet HX was used on the coolant side. The heat exchangers were made of aluminum to maintain uniform temperature along both sides of the TEGs. The heat exchanger was integrated with 48 TEG modules, split into 2 rows with 24 TEGs each, sandwiched between both HXs. The TEGs in each row are divided equally into 2 groups which are connected electrically together in parallel, all rows in the heat exchanger are connected electrically in series. Flat TEGs (Model number: TEG1-12610-5.1) [33] were used with dimensions 40 mm × 40 mm and a maximum power of 5.1 W per TEG at a hot-side temperature of 300 °C and a cold-side temperature of 30 °C. A brief description of the experimental test facility is provided in Appendix A. All the parameters of the TEGs and the HXs that were used in the experimental testing are presented in Table 1 [26,32]. The thermal resistances in the thermal network are calculated based on the heat exchanger operation and design parameters provided in Table 1.

The inlet temperature of the exhaust gas is assumed to be constant

Table 1
Design and operation parameters of the multi-row TEG-HX system [26,32].

Parameter [unit]	Value
TEGs characterization effective parameters [26]	
Per TEG:	
• Seebeck coefficient (α_T) $[V/K]$	0.0346
• Internal electrical resistance (r_T) $[ohm]$	3.07
• Thermal conductance (K_T) $[W/K]$	0.614
HX operation parameters [26,32]	
Gas inlet:	
• Temperature $[^{\circ}C]$	270
• Mass flow rate ($\dot{m}_g$) $[kg/s]$	0.02 – 0.08
Water inlet:	
• Temperature $[^{\circ}C]$	8
• Mass flow rate per row ($\dot{m}_{water}$) $[kg/s]$	0.0345
HX design parameters [26,32]	
Material: Aluminum	
• Thermal conductivity (λ) $[W/m{\cdot}K]$	200
TEGs (per row):	
• Number of modules	24
Rows Thermal modeling [26]	
Hot-side:	
• Nusselt number [34] for laminar flow in rectangular channels with aspect ratio (α^*)	6.41
• Transverse thermal resistance ($R_{th,HX,H}$) $[K/W]$	0.0154
• Axial thermal resistance ($R_{th,A,H}$) $[K/W]$	0.0194
Cold-side:	
• Nusselt number [31]	$0.3276Re^{0.4225}Pr^{1/3}$
• Transverse thermal resistance ($R_{th,HX,C}$) $[K/W]$	0.0126
• Axial thermal resistance ($R_{th,A,C}$) $[K/W]$	0.0454

since the outlet temperature of the oven depends on the oven setpoint temperature [32]. The exhaust mass flow rate is set to vary in the range of 0.02 to 0.08 kg/s which lies in the range of operation of similar commercial ovens depending on the draft conditions. The water inlet temperature and mass flow rate per row are kept constant and the total flow rate of water to the heat exchanger is equal to the number of TEG rows multiplied by a constant water flow rate per row. For the studied range of the exhaust gas flow rate, Reynolds number (Re) is found to be lower than 500, and thus the Nusselt number correlation for laminar flow is used [34]. The maximum uncertainty in the experimental measurements are ±1.9 °C for the exhaust gas temperature, ±0.13 °C for the water temperature, ±0.001 kg/s for the exhaust gas mass flow rate, ±0.0003 kg/s for the water mass flow rate and ±0.25 W for the power output.

The numerical and experimental steady-state results are compared under the testing conditions outlined in Table 1. The numerical results for the gas and water outlet temperatures and the TEG hot- and cold-side temperatures show good agreement with the experimental results with a maximum error of 6% in the outlet temperature of the exhaust gas, Figs. 4 and 5. By increasing the exhaust gas mass flow rate, the hot-side temperature of the TEGs increases due to the increase in the available thermal energy in the exhaust flow. This also results into an increase in the temperature of the exhaust gas, shown in Fig. 4, and the heat flow through the heat exchanger. The deviation in the predicted gas outlet temperature from the experimental data may be attributed to the one-dimensional treatment of the gas and HX base temperatures in the normal direction to the flow and the use of an average Nusselt number to estimate the gas heat transfer coefficient. Such deviation could be improved using two-dimensional modeling of the gas flow [26]. It is worth mentioning that the plotted hot-side temperature of the TEGs is calculated as an average value at the center while the gas

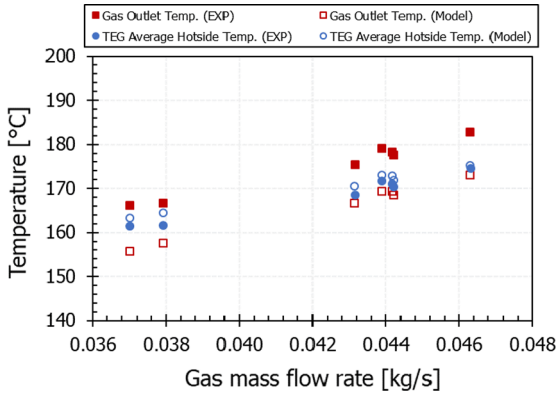

Fig. 4. Comparison between experimental and numerical results for gas outlet temperature and TEG hot-side temperature under different gas flow rates [26].

temperature is at the outlet of each TEG row. The cold-side of the TEGs experiences a slight increase in temperature due to the larger heat capacity of water ($\dot{m}C_w$) compared to that of the exhaust gas, Fig. 5.

General agreement is also noticed between the results for the power output and efficiency, shown in Fig. 6. By neglecting the effect of the axial conduction (NAC) along the heat exchanger, the model overestimates the TEG power output and a larger deviation from the experimental data is observed. This indicates that accounting for the effect of the axial conduction between the TEG rows in the numerical model is essential for the accurate prediction of the power output. The power output of the TEGs is found to increase by around 10% with the increase of the gas mass flow rate from 0.038 to 0.044 kg/s due primarily to the increase of the temperature difference across the TEGs (Figs. 4 and 5). The efficiency, however, shows a smaller increase of around 5%. In theory, the power output of the TEGs is directly proportional to the square of the temperature difference across the TEG, whereas the efficiency is linearly proportional to the temperature difference across the TEG [1].

Despite the increase in the power output and efficiency over the tested range of exhaust mass flow rates, there is a noticeable deviation in the power output data points in Fig. 6 at approximately 0.037 and 0.046 kg/s. This deviation could be due to the error in the exhaust gas mass flow rate measurements.

4. Results and Discussion

The performance of a TEG-HX waste heat recovery system is affected by various operation and design parameters. This study focuses on the effect of varying the exhaust mass flow rate as well as the effect of the axial heat conduction between consecutive rows of TEGs due to the heat exchanger design. The validated TEG-HX numerical model is used for this study.

4.1. Effect of operation and design parameters of the heat exchanger

The mass flow rate of the exhaust gas can significantly affect the performance of the TEG-HX waste heat recovery system. The effect is primarily pronounced in the streamwise temperature distribution of the exhaust gas stream. This, in turn, will impact the hot-side temperature of the TEG rows in the direction of the gas flow. A TEG-HX system, consisting of two consecutive TEG rows, operating under the conditions listed in Table 1, is investigated. The length of the TEG row in the axial direction is chosen to be 63 mm. Fig. 7 shows that the decrease of the

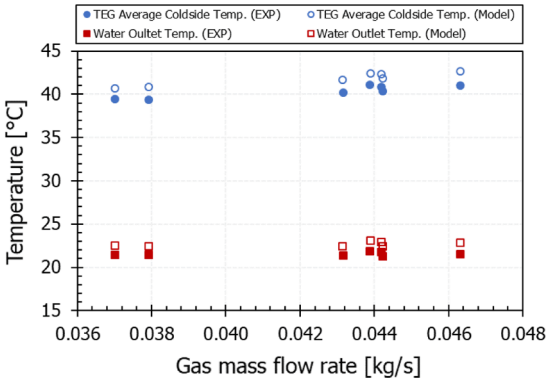

Fig. 5. Comparison between experimental and numerical results for water outlet temperature and TEG cold-side surface temperature under different gas flow rates [26].

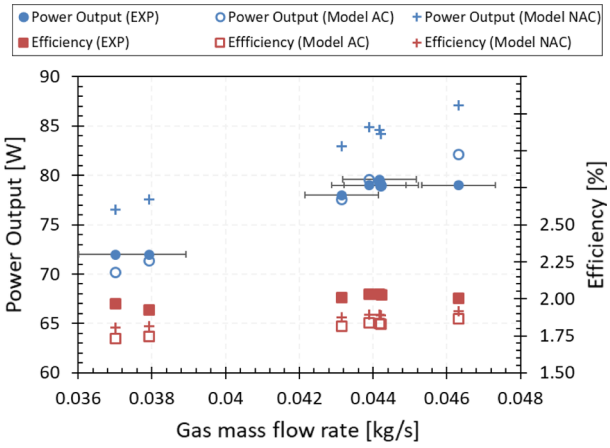

Fig. 6. Comparison between experimental and numerical results for power output and efficiency under different gas flow rates [26].

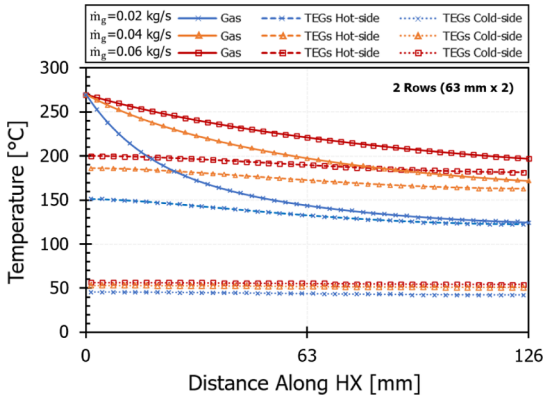

Fig. 7. Temperature distribution along the heat exchanger length for different exhaust gas mass flow rates.

exhaust flow rate yields larger axial temperature gradient in the exhaust gas due primarily to the increase in the heat exchanger effectiveness. This is found to have a prominent effect on the total power output from the TEGs, as illustrated in Fig. 8. Larger temperature gradients in the exhaust gas results into lower temperature on the hot-side of the TEG, and hence lower power output from the TEGs.

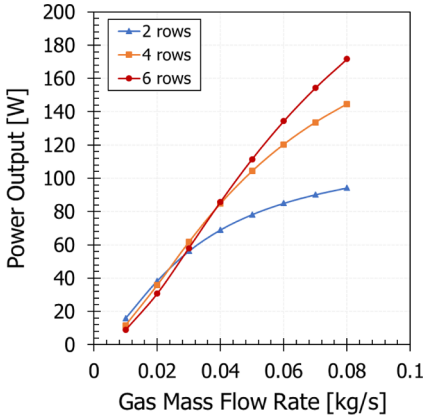

Fig. 8. The variation of TEGs maximum total power output under different exhaust gas mass flow rates for different heat exchanger sizes.

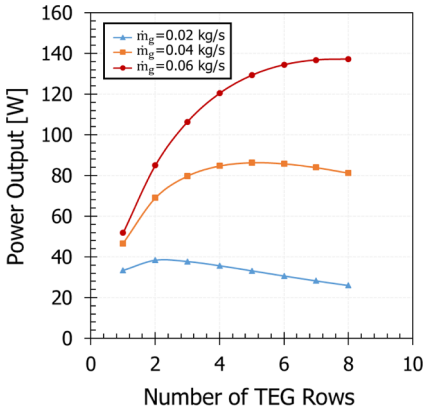

Fig. 9. The effect of the number of TEG rows on the total power output under different exhaust gas mass flow rates.

The number of the TEG rows have a significant effect on the performance of the waste heat recovery system. Increasing the size of the heat exchanger to include more TEG rows yields larger power output at higher gas mass flow rates (greater than0.03 kg/s). However, for lower gas flow rates (less than0.02 kg/s), two rows of TEGs is found to generate a slightly higher power compared to that with four and six rows. Fig. 9 shows that as the exhaust gas flow rate increases, the maximum total power output occurs at a larger number of TEG rows. This is due to the increase in the average hot-side temperature of the TEGs, shown in Fig. 7. This indicates that more rows can be added as the gas flow rate increases since more energy will be available for more TEG rows downstream. The maximum total power output of the TEGs is found to occur at 5 and 7 rows for the gas mass flow rates of 0.04 and 0.06 kg/s, respectively. Also, Fig. 9 illustrates that the power output from the system with a gas flow rate of 0.02 kg/s peaks when the number of TEG rows is two. This can be explained by looking at the average hot-side temperature of each TEG row shown in Fig. 10. For the case of low gas flow rate and large number of rows, the temperature difference between the hot-side and cold-side of the TEG rows downstream are considerably lower than those of the TEG rows upstream. Despite the increase in the total number of TEGs, such behavior can lead to significant deterioration of the power output from the system due to the temperature mismatch [35].

Consider Fig. 11 which shows the performance curves of a 6-row

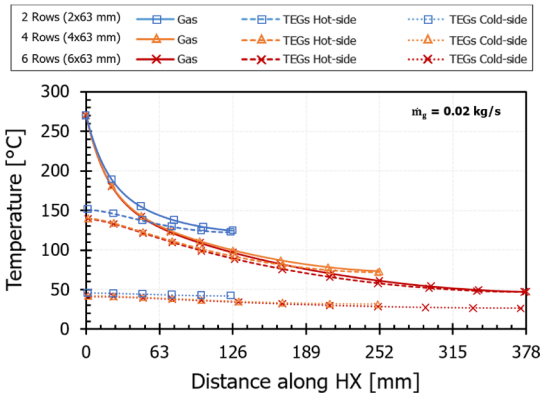

Fig. 10. The temperature distribution along the heat exchanger length for different number of TEG rows at constant exhaust gas mass flow rate of 0.02 kg/s.

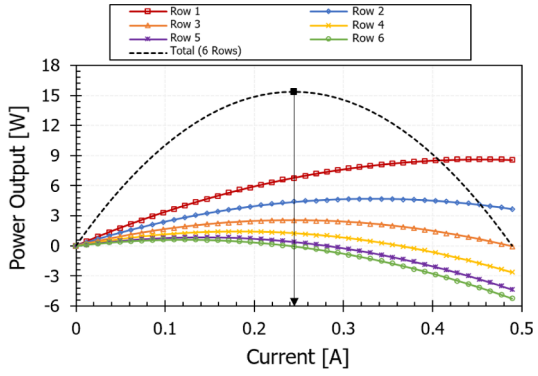

Fig. 11. The power output of TEGs versus current output in a heat exchanger of consisting of 6 TEG rows with exhaust gas flow rate of 0.02 kg/s.

system with low gas flow rate (0.02 kg/s) connected electrically in series. The total power is maximized when all six TEG rows are operating at approximately 0.245 A. Due to the large temperature mismatch, the high temperature upstream TEG rows are found to be operating off their peak power point causing a significant drop in the total power of the system. It is seen that under certain operating conditions the TEG rows downstream can start acting as heat pumps instead of heat engines (i.e., consume electric power instead of generating due to the large mismatch in temperatures between the TEG rows). This penalizes the whole system by lowering the total output power. As a result, such systems should be operated at lower electric currents to maximize the total power output. However, this would sacrifice the operation of the upstream TEG rows at their individual maximum power output. The adverse effect of the temperature mismatch in this system of TEGs can be mitigated by maximizing the power output of each TEG row using individual power management circuits. However, this might lead to a more complicated and expensive power management system.

4.2. Effect of axial conduction on TEGs performance

The results presented in the previous section show that, for a given heat exchanger design, an optimum number of TEG rows is needed to maximize the total power output of the system depending on the

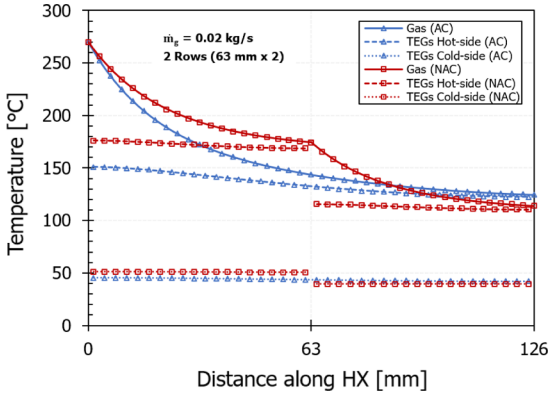

Fig. 12. Temperature distribution along the heat exchanger length for two rows of TEGs and exhaust gas mass flow rate of 0.02 kg/s for AC and NAC cases.

exhaust gas mass flow rate. This section focuses on evaluating the effects of the axial conduction on the power output of the multi-row TEG-HX waste heat recovery systems. Axial conduction (AC) of heat takes place through the structure of the heat exchangers on the hot- and cold-side of the TEGs between the consecutive rows. High temperature rows near the gas inlet transfers heat by conduction to lower temperature rows near the gas outlet as the exhaust gas cools through the heat exchanger. The axial conduction causes the temperature of the hot- and cold-sides of the TEGs to have a lower gradient along the direction of the exhaust gas flow, which will have a significant impact on the overall power output of the system. The temperature profiles and power output are compared in the case when the axial conduction (AC) is considered versus the case where no axial conduction (NAC) takes place between the TEG rows. Practically, the effect of axial heat conduction between neighboring rows can be limited by introducing air gaps or adding thin insulation layers between the rows.

4.2.1. Effect of axial conduction on temperature profiles

The effect of the axial conduction is eliminated artificially in the numerical simulations by thermally insulating between consecutive TEG rows in the axial direction, i.e. setting the thermal conductance values $K_{A,H}$ and $K_{A,C}$ to zero. Fig. 12 shows the effect of axial conduction on the temperature profiles along the heat exchanger length for an exhaust flow rate of 0.02 kg/s. It is seen that the gas temperature in the case with no axial conduction (NAC) shows higher temperature values at the outlet of the first row and a lower temperature value at the outlet of the second row. This indicates larger amount of heat recovered from the exhaust gas when the TEG rows are thermally isolated from one another.

In addition, the first row of TEGs experiences significantly higher temperature in the NAC case compared to the AC case, whereas the second row has a slightly lower temperature. The axial temperature gradient on the hot-side of the TEG is found to be generally lower in the case of NAC. Due to the relatively large water mass flow rate, the cold-side temperatures of both rows are seen to be hardly affected with slight changes in temperature compared to the TEGs hot-side.

For a given exhaust mass flow rate, Fig. 13 shows that the axial heat conduction acts to reduce the hot-side temperature of the upstream TEGs and increase that of the downstream TEGs. As such, the system with NAC experiences a higher temperature differences across the upstream TEG rows compared to the case with AC. This is observed to be of high importance in applications with low exhaust gas mass flow rate,

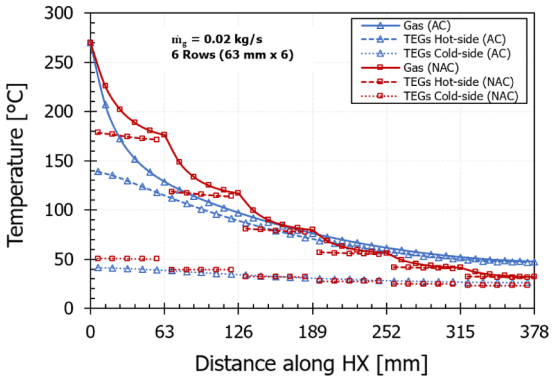

Fig. 13. Temperature distribution along the heat exchanger length for six rows of TEGs and exhaust gas mass flow rate of 0.02 kg/s for AC and NAC cases.

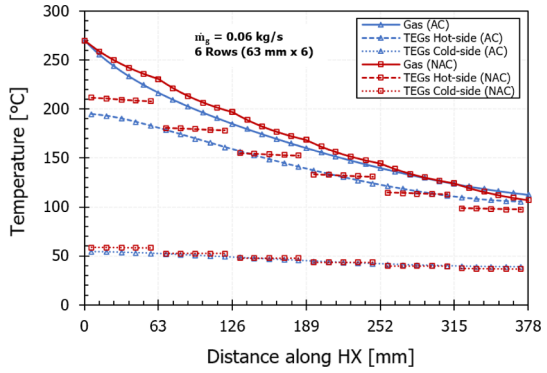

Fig. 14. Temperature distribution along the heat exchanger length for six rows of TEGs and exhaust gas mass flow rate of 0.06 kg/s for AC and NAC cases.

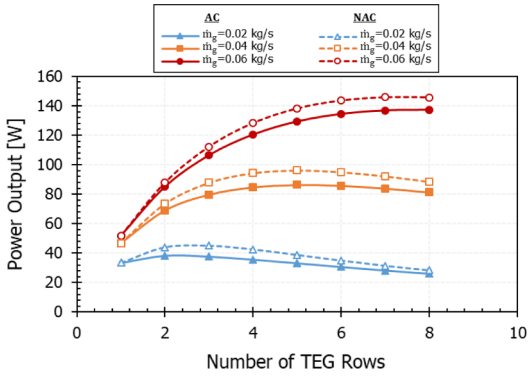

Fig. 15. Comparison of the TEGs total power output under different exhaust gas mass flow rates and number of TEG rows for AC and NAC cases.

since the gas undergoes a large temperature drop near the inlet. By limiting the axial conduction between the TEG rows, more power can potentially be generated from the upstream TEG rows.

By increasing the exhaust gas mass flow rate for a given number of TEG rows, Fig. 14 shows that the temperature profiles of both cases with AC and NAC relatively approach each other since the high flow rate promotes a more uniform temperature distribution through the heat exchanger. Nevertheless, the case with NAC still shows a slightly higher temperature difference across the TEGs in the rows upstream than the AC case.

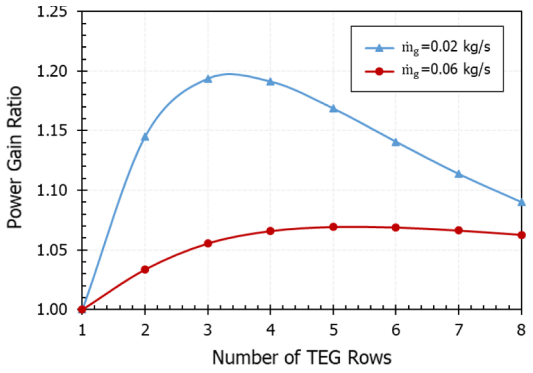

Fig. 16. Power Gain for different exhaust gas mass flow rates and number of TEG rows.

4.2.2. *Effect of axial conduction on TEGs power output*

Since the power output is directly proportional to the square of the temperature difference across the TEG [1], the temperature distributions on the hot- and cold-sides of the TEGs have a significant effect on the overall power output of the TEGs. As shown in Fig. 14, the axial conduction of heat between the TEG rows causes the temperature of the first row to drop significantly compared to the subsequent rows. This is expected to have an adverse effect on the total power output from the system. Fig. 15 presents the power output from the TEGs operating under different exhaust gas mass flow rates and number of rows for both cases with AC and NAC. The power output is found to be higher in case with NAC compared to the case with AC for all cases illustrated in Fig. 15. This highlights the advantage of thermally insulating between the consecutive rows in TEG-HX systems. The increase in the power output is mainly due to the significant increase in temperature of the upstream rows which prevailed in all the cases with NAC. For the studied range of gas flow rate, the number of rows that maximizes the power output from the TEGs was found to be independent of the effect of the axial heat conduction through the heat exchangers.

As a result, a new term “Power Gain” is introduced herein as the ratio of the power generated from the TEGs in the case of no axial conduction (NAC) to the case with axial conduction (AC) for the same heat exchanger design operating under the same conditions:

$$Power\ \ Gain = \frac{P_{NAC}}{P_{AC}} \tag{11}$$

The Power Gain is calculated using Eq. (11) and plotted in Fig. 16 against different number of TEG rows for exhaust gas mass flow rates of 0.02 kg/s and 0.06 kg/s. It is seen that the Power Gain is always higher than unity, which indicates that the case with NAC generates higher power output than that with AC. Limiting the effect of the axial

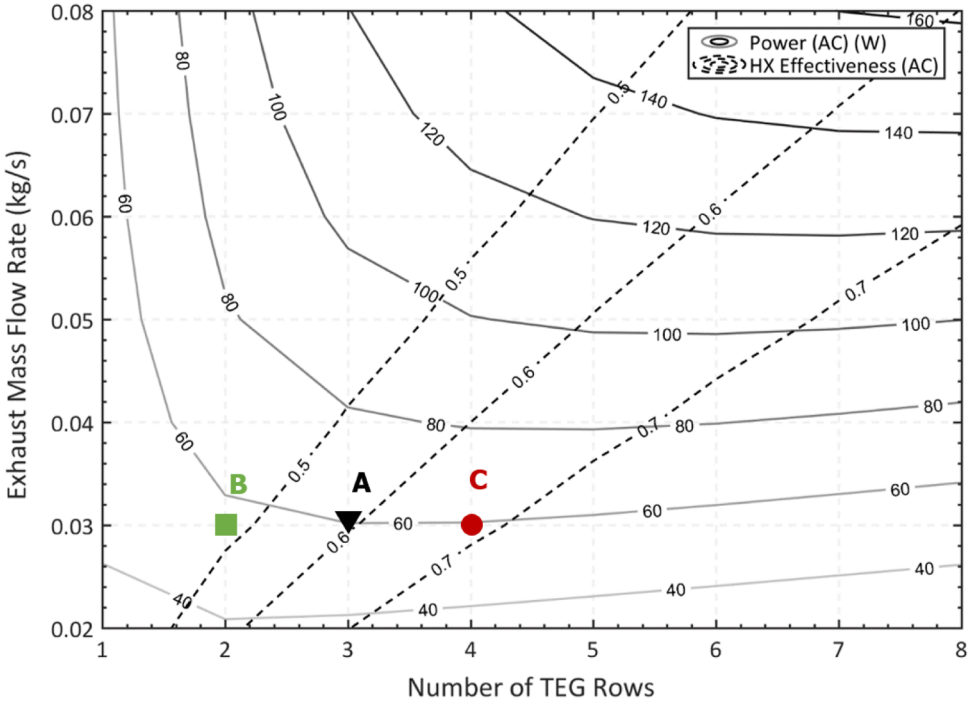

Fig. 17. TEGs total power output and heat exchanger effectiveness for AC case with different number of TEG rows and exhaust gas mass flow rates.

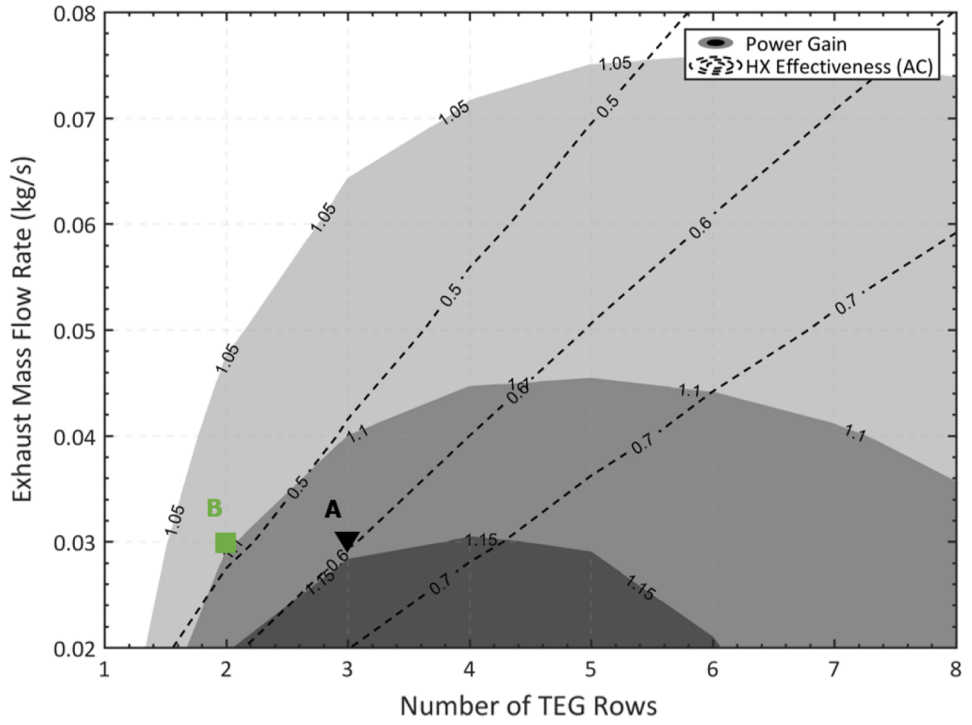

Fig. 18. TEGs Power Gain and heat exchanger effectiveness for different number of TEG rows and exhaust gas mass flow rates.

conduction is found to be more effective in the cases with lower exhaust gas flow rates due primarily to the larger increase in the temperature difference across the TEGs upstream.

As the number of rows increases, the value of the Power Gain reaches a maximum value then drops. This means that there exists an optimum design for the case with NAC beyond which increasing the

heat exchanger size and adding more TEG rows becomes less beneficial. This is because the available energy in the exhaust gas becomes insufficient for the added TEGs to generate more power. As such, it is seen that limiting the axial heat conduction in such systems can offer a great potential of reducing the size of the heat exchangers, the number of TEGs needed, and hence the cost of the entire system. It is worth mentioning, however, that despite such advantages, the means of limiting the axial conduction between the TEG rows might present technical and economic complexities on the design of the heat exchangers. Such factors are considered outside the scope of the current study.

4.3. Design criteria for TEG-HX

As previously illustrated, the performance of the multi-row TEG-HX waste heat recovery system is a function of various parameters such as the number of rows (i.e., the size of the heat exchanger), the number of TEGs per row, and the exhaust mass flow rate. For certain applications with limited exhaust flow rate such as commercial ovens, the heat exchangers of the waste heat recovery system must be carefully sized to maximize the power output.

The effectiveness of the heat exchanger is a useful design parameter that can practically link the size of the heat exchanger to the amount of heat transferred through it. The effectiveness (ϵ) is defined as the rate of heat transferred through the heat exchanger to the maximum heat transfer rate [36]:

$$\epsilon = \frac{C_h(T_{h,i} - T_{h,o})}{C_{min}(T_{h,i} - T_{c,i})} = \frac{\dot{m}_g C_{p,g}(T_{g,in} - T_{g,out})}{\dot{m}_g C_{p,g}(T_{g,in} - T_{w,in})} \quad (12)$$

The heat exchanger effectiveness is calculated for the previously studied design with axial conduction (AC) to investigate the relationship between the effectiveness and the power output from the TEGs. For a range of exhaust gas mass flow rates from 0.02 to 0.08 kg/s and a number of rows from 1 to 8 rows, the numerical results are presented in a 2D Power Output map, Fig. 17. It is seen that the heat exchanger effectiveness can be used as a design criterion to identify the maximum power for any given exhaust gas flow rate, and hence guides the selection of the appropriate number of TEG rows needed.

To help clarify this, consider an example of the multi-row TEG-HX waste heat recovery system, described in Appendix A, operating with an exhaust flow rate of 0.03 kg/s. A heat exchanger with 60% effectiveness will require three TEG rows to maximize the output power (Design A in Fig. 17). However, a heat exchanger with lower effectiveness (Design B: 47% effectiveness with 2 TEG rows) will lead to a 6% decrease in the power output but a more compact design with a smaller number of TEGs. Finally, choosing a heat exchanger with higher effectiveness (Design C: 68% effectiveness with 4 TEG rows) will result in little to no increase in the power output (within 1%), which might not justify the increased number of TEGs.

The Power Gain by eliminating the axial conduction can also be used as a critical design criterion to guide the decision of thermally insulating between successive TEG rows. Fig. 18 illustrates a 2D Power Gain map of the gain values for a range of exhaust gas mass flow rates from 0.02 to 0.08 kg/s and number of rows from 1 to 8 rows. It is shown that higher values of Power Gain (more than 1.15) occur at lower exhaust flow rates (less than 0.03 kg/s). Comparing Design A and B in Fig. 18, it is found that for an exhaust gas mass flow rate of 0.03 kg/s, Design A has a larger Power Gain of 1.14 (i.e., 14% enhancement) compared to Design B with a Power Gain of around 1.1 (i.e., 10% enhancement). This demonstrates that the decision of limiting the axial conduction in Design A will be of greater value than in Design B.

5. Conclusion

The design of a heat exchanger for waste heat recovery applications requires certain considerations when thermoelectric generators (TEGs) are integrated within the design. Such considerations provide design criteria for integrating TEGs in a heat exchanger to achieve the objective of maximizing the power output from the TEGs. The effects of the heat exchanger operation and design parameters such as the exhaust gas mass flow rate and number of TEG rows on the power output of TEGs are studied. Since the performance of the system is highly dependent on the temperature difference across the TEGs, accurate modeling of the coupling between heat transfer and the thermoelectric effects is required. As such, a numerical model is developed and then experimentally validated to simulate the performance of a multi-row TEG-HX design. The model takes into consideration the effect of the temperature distribution along the heat exchanger, the electrical connection and the axial conduction between TEG rows.

The numerical results show that the power output increases with the exhaust gas flow rate. However, for a given gas flow rate, there exists an optimum number of TEGs to maximize the power output from the system. The axial conduction between consecutive TEG rows is found to have an adverse effect on the total power output since it decreases the temperature difference across the higher temperature TEGs near the heat exchanger inlet resulting in lower power generation. The term “Power Gain” is defined as the ratio between the power output from a TEG-HX design without axial conduction to that from a design with axial conduction. The Power Gain is always found to be higher than unity for different exhaust gas mass flow rates and number of TEG rows. The numerical results show that higher Power Gain values can be obtained at low exhaust gas mass flow rates; up to 1.2 times for the case with gas flow rate of 0.02 kg/s. The heat exchanger effectiveness is also found to be a valuable tool to guide the sizing of the heat exchanger for maximum system power output. The Power Gain and the heat exchanger effectiveness can be used as design criteria to evaluate the potential benefits of limiting the axial heat conduction at the design stage of TEG-HX systems. The Power Output and Gain maps are used in a case study of a two-row experimental heat exchanger to guide designers through the optimization of the number of TEG rows in the heat exchanger and the prediction of the gain in the power output obtained by eliminating the axial conduction. The proposed performance maps suggest that three TEG-rows provide the optimum performance for the studied system with significant enhancement of 14% in the power output due to eliminating the axial conduction between the rows.

CRediT authorship contribution statement

M.H. Zaher: Methodology, Software, Validation, Investigation, Data curation, Formal analysis, Writing - original draft. **M.Y. Abdelsalam:** Data curation, Formal analysis, Visualization, Writing - review & editing. **J.S. Cotton:** Conceptualization, Supervision, Funding acquisition, Writing - review & editing.

Declaration of Competing Interest

The authors declare that they have no known competing financial interests or personal relationships that could have appeared to influence the work reported in this paper.

Acknowledgements

The authors are thankful for the support and funding provided by the Natural Sciences and Engineering Research Council of Canada (NSERC) and the Ontario Centres of Excellence (OCE).

Appendix A. – The experimental test setup of TEG-integrated heat exchanger

The experimental test setup is described in detail in previous work by Girard [32] and Zaher [26]. It is comprised of a natural gas commercial oven with a TEG-integrated heat exchanger mounted between the oven and the chimney as shown in Fig. A1. The cooling water is supplied to the heat exchanger cold side from the main supply, while the exhaust is supplied to the hot side of the heat exchanger from the oven. Fig. A2 shows a schematic of the TEG-integrated heat exchanger with plate-fin HX in the exhaust side, the water side HX and the TEG arrangement. More details on the experimental facility and the uncertainties of the measurement devices are described by Zaher [26].

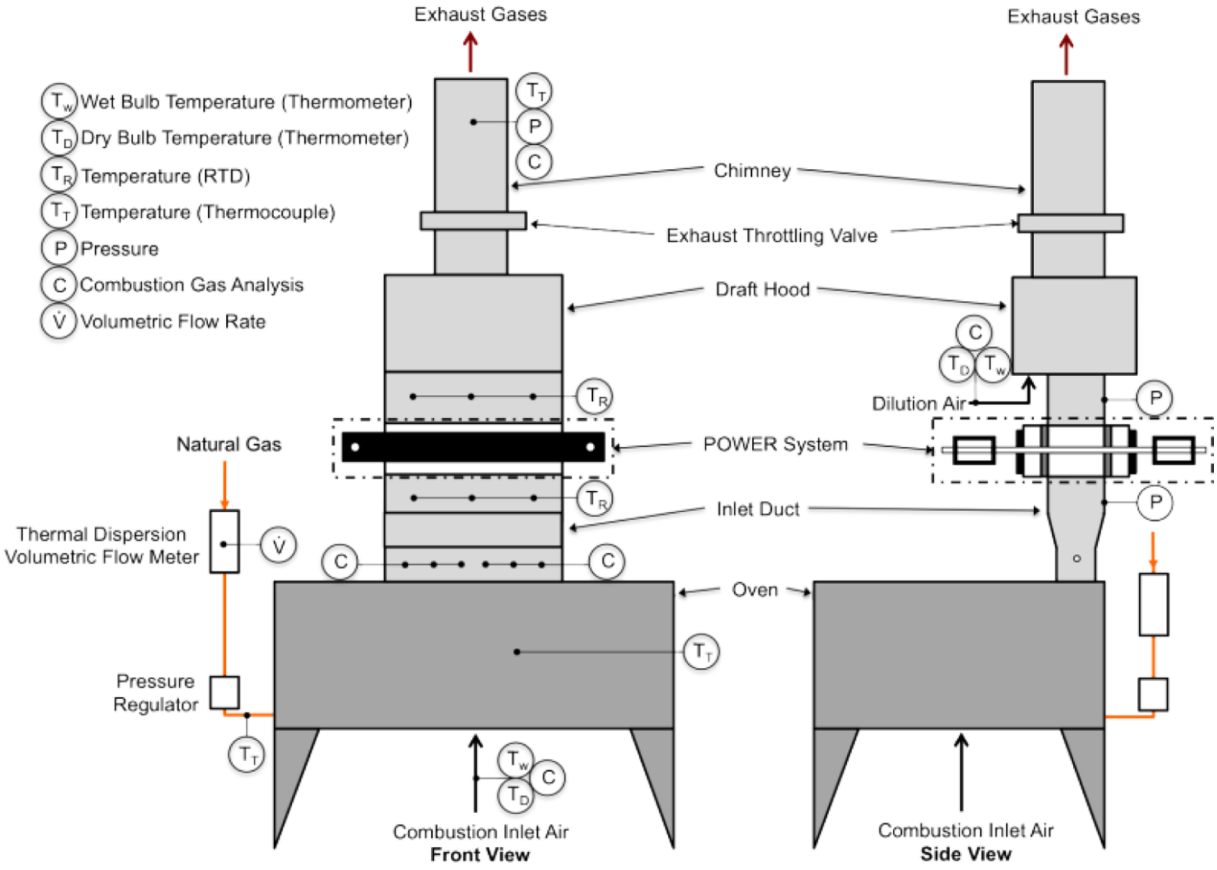

Fig. A1. Schematic of the TEG-HX testing facility [32].

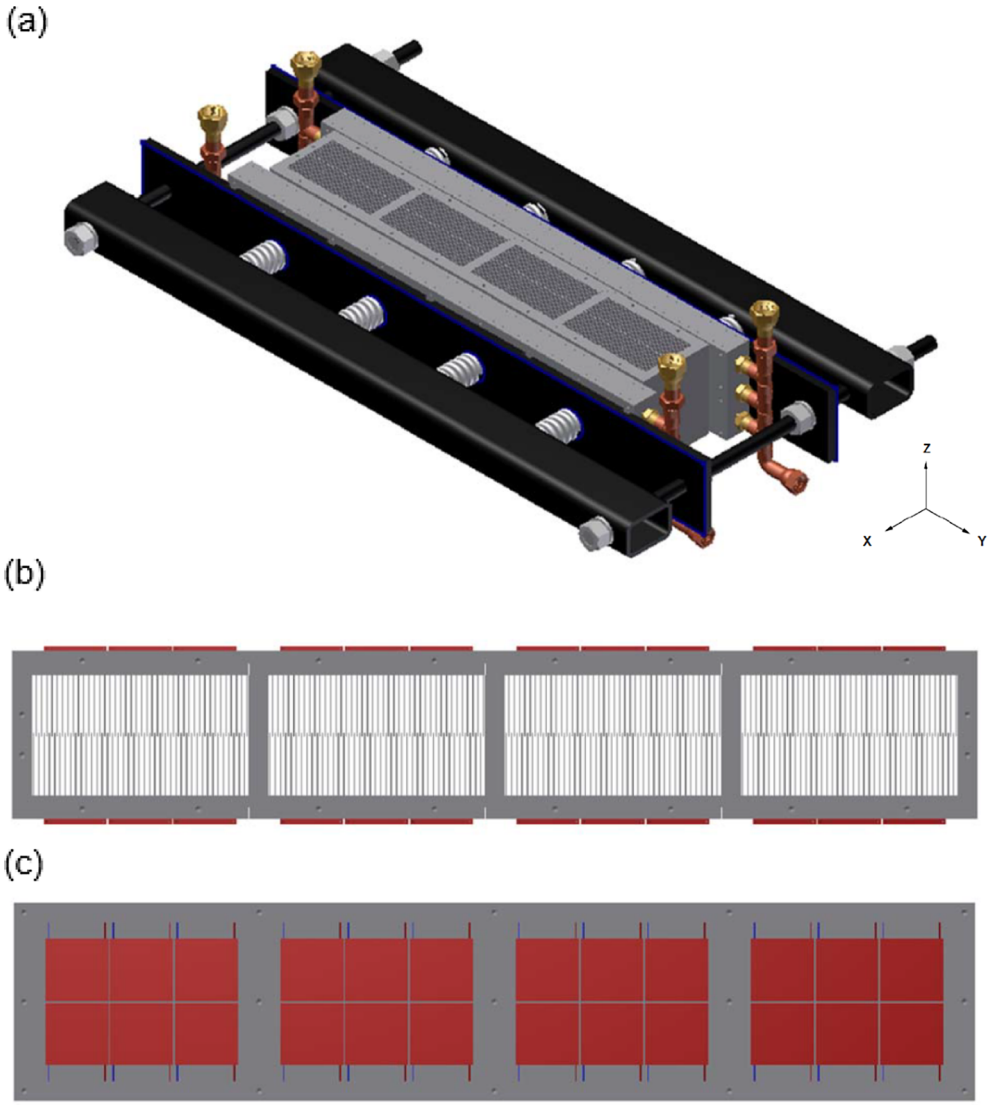

Fig. A2. (a) Schematic of the TEG-integrated heat exchanger – (b) Top view of the exhaust side plate-fin HX – (c) TEG modules attached to the HX base [26].

References

[1] Rowe D, editor. Thermoelectrics Handbook: macro to nano. CRC Press; 2005. http://doi.org/10.1201/9781420038903.

[2] Ioffe AF, Stil'bans LS, Iordanishvili EK, Stavitskaya TS, Gelbtuch A, Vineyard G. Semiconductor thermoelements and thermoelectric cooling. Phys Today 1959;12:42-42. https://doi.org/10.1063/1.3060810.

[3] Goldsmid HJ. Conversion efficiency and figure-of-merit. CRC Handb Thermoelectr 1995:32–9. https://doi.org/10.1201/9781420049718.ch3.

[4] Cobble MH. Calculations of generator performance. CRC Handb Thermoelectr 1995;2:489–92. https://doi.org/10.1201/9781420049718.ch39.

[5] Lau P, Buist R. Calculation of thermoelectric power generation performance using finite element analysis. XVI ICT '97 Proc ICT'97 16th Int Conf Thermoelectr (Cat No97TH8291) 1997. p. 563–6. https://doi.org/10.1109/ICT.1997.667592.

[6] Fraisse G, Ramousse J, Sgorlon D, Goupil C. Comparison of different modeling approaches for thermoelectric elements. Energy Convers Manag 2013;65:351–6. https://doi.org/10.1016/j.enconman.2012.08.022.

[7] Henderson J. Analysis of a heat exchanger-thermoelectric generator system. 14th Intersoc Energy Convers Eng Conf, 2. 1979. p. 1835–40.

[8] Stevens JW. Optimal design of small DT thermoelectric generation systems. Energy Convers Manage 2001;42:709–20. https://doi.org/10.1016/S0196-8904(00)00099-6.

[9] Min G, Rowe DM. Optimisation of thermoelectric module geometry for "waste heat" electric power generation. J Power Sources 1992;38:253–9. https://doi.org/10.1016/0378-7753(92)80114-Q.

[10] Rowe D, Min G. Peltier devices as generators. CRC Handb Thermoelectr CRC Press; 1995. https://doi.org/10.1201/9781420049718.ch38.

[11] Rowe DM, Min G. Evaluation of thermoelectric modules for power generation. J Power Sources 1998;73:193–8. https://doi.org/10.1016/S0378-7753(97)02801-2.

[12] Rowe DM, Min G. Design theory of thermoelectric modules for electrical power generation. IEE Proc-Sci, Meas Technol 1996;143:351–6. https://doi.org/10.1049/ip-smt:19960714.

[13] Glatz W, Muntwyler S, Hierold C. Optimization and fabrication of thick flexible polymer based micro thermoelectric generator. Sens Actuat, A Phys 2006;132:337–45. https://doi.org/10.1016/j.sna.2006.04.024.

[14] Strasser M, Aigner R, Franosch M, Wachutka G. Miniaturized thermoelectric generators based on poly-Si and poly-SiGe surface micromachining. Sens Actuat, A Phys 2002;97–98:535–42. https://doi.org/10.1016/S0924-4247(01)00815-9.

[15] Freunek M, Reindl LM, Walker WD. Modified model for thermoelectric generators. Ect 2008;2008(49):1–4.

[16] Freunek M, Müller M, Ungan T, Walker W, Reindl LM. New physical model for thermoelectric generators. J Electron Mater 2009;38:1214–20. https://doi.org/10.1007/s11664-009-0665-y.

[17] Kumar S, Heister SD, Xu X, James R, Meisner GP. Thermoelectric generators for automotive waste heat recovery systems Part I: Numerical modeling and baseline model analysis. J Electron Mater 2013;42:665–74. https://doi.org/10.1007/s11664-013-2471-9.

[18] Kumar S, Heister SD, Xu X, Salvador JR, Meisner GP. Thermoelectric generators for automotive waste heat recovery systems part II: Parametric evaluation and topological studies. J Electron Mater 2013;42:944–55. https://doi.org/10.1007/s11664-013-2472-8.

[19] Crane DT, Jackson GS, Holloway D. Towards Optimization of Automotive Waste Heat Recovery Using Thermoelectrics. Therm. Syst. Manag. geat Exch. SAE International; 2001. p. 53–66.

[20] Crane DT, Jackson GS. Optimization of cross flow heat exchangers for thermoelectric waste heat recovery. Energy Convers Manage 2004;45:1565–82. https://doi.org/10.1016/j.enconman.2003.09.003.

[21] Yu J, Zhao H. A numerical model for thermoelectric generator with the parallel-plate heat exchanger. J Power Sources 2007;172:428–34. https://doi.org/10.1016/j.jpowsour.2007.07.045.
[22] Niu X, Yu J, Wang S. Experimental study on low-temperature waste heat thermoelectric generator. J Power Sources 2009;188:621–6. https://doi.org/10.1016/j.jpowsour.2008.12.067.
[23] Gou X, Xiao H, Yang S. Modeling, experimental study and optimization on low-temperature waste heat thermoelectric generator system. Appl Energy 2010;87:3131–6. https://doi.org/10.1016/j.apenergy.2010.02.013.
[24] Hsu CT, Huang GY, Chu HS, Yu B, Yao DJ. Experiments and simulations on low-temperature waste heat harvesting system by thermoelectric power generators. Appl Energy 2011;88:1291–7. https://doi.org/10.1016/j.apenergy.2010.10.005.
[25] Meng J-H, Wang X-D, Chen W-H. Performance investigation and design optimization of a thermoelectric generator applied in automobile exhaust waste heat recovery. Energy Convers Manag 2016;120:71–80. https://doi.org/10.1016/j.enconman.2016.04.080.
[26] Zaher M. The integration of annular thermoelectric generators in a heat exchanger for waste heat recovery applications. McMaster University; 2017.
[27] Huang G, Hsu C, Fang C, Yao D. Optimization of a waste heat recovery system with thermoelectric generators by three-dimensional thermal resistance analysis. Energy Convers Manage 2016;126:581–94. https://doi.org/10.1016/j.enconman.2016.08.038.
[28] Wang Y, Dai C, Wang S. Theoretical analysis of a thermoelectric generator using exhaust gas of vehicles as heat source. Appl Energy 2013;112:1171–80. https://doi.org/10.1016/j.apenergy.2013.01.018.
[29] Love ND, Szybist JP, Sluder CS. Effect of heat exchanger material and fouling on thermoelectric exhaust heat recovery. Appl Energy 2012;89:322–8. https://doi.org/10.1016/j.apenergy.2011.07.042.
[30] Finnerty D. The development of methodologies and a novel test facility for the characterisation of thermoelectric generators. McMaster University; 2013.
[31] Hana Y. Characterization of Flat-Plate Heat Exchangers for Thermal Load Management of Thermoelectric Generators. McMaster University; 2014.
[32] Girard J. The investigation of exhaust control strategies and waste heat recovery practices of naturally-ventilated exhaust streams. McMaster University; 2016.
[33] TECTEG/Thermal-Electronics. Specifications TEG Module TEG1-12610-5.1 2016:2. http://tecteg.com/wp-content/uploads/2014/09/1.pdf.
[34] Kakaç S, Shah RK, Aung W, editors. Handbook of single-phase convective heat transfer. New York: Wiley; 1987. c1987.
[35] Montecucco A, Siviter J, Knox AR. The effect of temperature mismatch on thermoelectric generators electrically connected in series and parallel. Appl Energy 2014;123:47–54. https://doi.org/10.1016/j.apenergy.2014.02.030.
[36] Incropera FP, DeWitt DP, Bergman TL, Lavine AS. Fundamentals of Heat and Mass Transfer. John Wiley & Sons; 2007. vol. 6th http://doi.org/10.1016/j.applthermaleng.2011.03.022.